2-2015

Characterization of Sequential Collagen-Poly(Ethylene Glycol) Diacrylate Interpenetrating Networks and Initial Assessment of Their Potential for Vascular Tissue Engineering

Dany J. Munoz Pinto
Trinity University, dmunozpi@trinity.edu

Andrea C. Jimenez-Vergara
Trinity University, ajimene1@trinity.edu

T. P. Gharat

M. S. Hahn

HHS Public Access

Author manuscript

Biomaterials. Author manuscript; available in PMC 2017 June 13.

Published in final edited form as:

Biomaterials. 2015 February ; 40: 32–42. doi:10.1016/j.biomaterials.2014.10.051.

Characterization of Sequential Collagen-Poly(ethylene glycol) Diacrylat Interpenetrating Networks and Initial Assessment of their Potential for Vascular Tissue Engineering

Dany J. Munoz-Pinto, PhD[1], **Andrea Carolina Jimenez-Vergara, PhD**[1], **Tanmay Gharat**[2], and **Mariah S. Hahn, PhD**[1,2,*]

[1]Department of Biomedical Engineering, Rensselaer Polytechnic Institute, 110 8th Street Troy, NY, 12180, USA

[2]Department of Chemical and Biological Engineering, Rensselaer Polytechnic Institute, 110 8th Street Troy, NY, 12180, USA

Abstract

Collagen hydrogels have been widely investigated as scaffolds for vascular tissue engineering due in part to the capacity of collagen to promote robust cell adhesion and elongation. However, collagen hydrogels display relatively low stiffness and strength, are thrombogenic, and are highly susceptible to cell-mediated contraction. In the current work, we develop and characterize a sequentially-formed interpenetrating network (IPN) that retains the benefits of collagen, but which displays enhanced mechanical stiffness and strength, improved thromboresistance, high physical stability and resistance to contraction. In this strategy, we first form a collagen hydrogel, infuse this hydrogel with poly(ethylene glycol) diacrylate (PEGDA), and subsequently crosslink the PEGDA by exposure to longwave UV light. These collagen-PEGDA IPNs allow for cell encapsulation during the fabrication process with greater than 90% cell viability via inclusion of cells within the collagen hydrogel precursor solution. Furthermore, the degree of cell spreading within the IPNs can be tuned from rounded to fully elongated by varying the time delay between the formation of the cell-laden collagen hydrogel and the formation of the PEGDA network. We also demonstrate that these collagen-PEGDA IPNs are able to support the initial stages of smooth muscle cell lineage progression by elongated human mesenchymal stems cells.

INTRODUCTION

Collagen hydrogels have been widely investigated as scaffolds for vascular tissue engineering due in part to the abundance of collagen in the vessel wall and due to the capacity of a range of cell types to elongate and spread within collagen networks [1–4] [5]. Yet, collagen networks also have critical shortcomings which limit their broader utility in

*Corresponding Author: Mariah S. Hahn, PhD, Rensselaer Polytechnic Institute, 110 8th Street, Troy, NY, 12180, USA, Department of Biomedical Engineering, Telephone: 979-739-1343, Fax: 518-276-4233, hahnm@rpi.edu.

vascular graft applications. For instance, L'Hereux *et al*. employed collagen hydrogels to form the medial layer of their engineered vascular grafts [2]. However, the encapsulated smooth muscle cells contracted the collagen gels by up to 70% within 4 days of culture. Although adult mesenchymal stem cells (MSCs) are increasingly used as a source of smooth muscle cells for tissue engineered vascular grafts [6–10], MSC-laden collagen hydrogels are also prone to cell-mediated compaction [11]. In addition, Weinberg and Bell noted that vascular grafts based on tubular collagen hydrogels were so highly distensible that they ruptured at very low pressures (< 10 mmHg) and that increasing the concentration of collagen had limited effect on hydrogel strength [4]. This restricted capacity to manipulate collagen hydrogel strength is also reflected in the relatively limited range of stiffnesses achievable with pure collagen hydrogels [12, 13]. Specifically, the elastic moduli of collagen hydrogels range from 1–100 Pa [14, 15], significantly less stiff than that of small-diameter vascular tissue (40–900 kPa) [16, 17]. Furthermore, collagen hydrogels have a tendency to undergo rapid cell-mediated degradation, which can be challenging to control and predict, and the thrombogenicity of collagen requires graft pre-endothelialization prior to deployment [4, 18].

To reduce the thrombogenicity of collagen, researchers have linked thromboresistant molecules, such as heparin and poly(ethylene glycol), to the collagen network with promising results [19, 20]. Similarly, several strategies have been employed to enhance collagen hydrogel stiffness, strength, and resistance to degradation and cell-mediated compaction. For instance, Girton *et al*. demonstrated that glycation can be used to stiffen and strengthen collagen networks [21]. Further studies have since demonstrated that glycation reduces collagen susceptibility to matrix metalloproteinase degradation [22]. In addition, glutaraldehyde, hexamethylene diisocyanate, cyanamide, and 1-ethyl-3-(3-dimethyl aminopropyl) carbodiimide (EDC) have each been examined in terms of their capacity to increase the mechanical properties and slow the degradation rate of collagen hydrogels [23]. However, these chemical treatments can also have unwanted side-effects. For instance, glutaraldehyde-treated tissues are prone to calcification, a situation which is undesirable for vascular graft applications [24].

To address the limitations of pure collagen hydrogels while avoiding the drawbacks of chemical crosslinking treatments, we propose to combine collagen hydrogels with a poly(ethylene glycol) diacrylate (PEGDA) hydrogel to form an interpenetrating network (IPN). IPNs comprised of two distinct polymer networks have recently been shown to result in increased hydrogel stability, stiffness, and strength relative to either single component network [25–28]. Importantly, the component networks often contribute to IPN properties in a synergistic, rather than simply an additive, manner [25, 26]. For instance, recent polyacrylamide-alginate IPNs [27, 28] demonstrate an elastic modulus, tensile strength, and strain at failure that exceed the sum of the corresponding properties of the individual networks.

In the present work, we combine a covalently-crosslinked PEGDA network with a physically-crosslinked collagen network. PEGDA was selected as the second component of this collagen-based IPN due to the established biocompatibility, low thrombogenicity, and resistance to cell-mediated compaction characteristic of PEGDA hydrogels [29–31]. In

addition, the degradation rate and mechanical properties of PEGDA hydrogels can be systematically tailored. Specifically, although pure PEGDA hydrogels degrade relatively slowly, their degradation rate can be modified by introduction of hydrolytically or enzymatically-degradable segments within the PEG network [32–36]. Similarly, the mechanical performance of PEGDA hydrogels can be tuned by varying the molecular weight (MW) and concentration of PEGDA in the hydrogel precursor solution [37, 38]. Given these properties, it is reasonable to assume that a collagen-based IPN which includes PEGDA as the second network may display improved thromboresistance, higher resistance to cell-mediated compaction, and an increased range of mechanical properties relative to pure collagen.

Most IPNs, including those previously formed from PEG and collagen [39], are fabricated by mixing the two component polymers followed by their simultaneous crosslinking into interwoven networks [25, 27, 28, 39]. Unfortunately, in the case of collagen-PEG IPNs, this fabrication approach forces cells encapsulated within the IPN to take on a rounded cell phenotype, despite the presence of collagen. This is due to the nanoscale mesh structure and slow degradation rate of pure PEGDA hydrogels [40]. We propose to circumvent this limitation by first forming the collagen hydrogel and then infusing this hydrogel with PEGDA. Subsequent exposure of the infused network to longwave UV light will result in the formation of a PEGDA network interlaced with the pre-formed collagen network. As shown schematically in Figure 1, the degree of cell spreading in the IPN network can be controlled by varying the time delay between collagen hydrogel formation and PEGDA infusion and polymerization. In the current work, we demonstrate that this hybrid natural-synthetic IPN retains the benefits of collagen in terms of enabling robust cell elongation while improving scaffold stiffness and strength as well as scaffold resistance to compaction and platelet adhesion. Furthermore, we show the ability of these collagen-PEGDA IPNs to support the initial stages of MSC progression toward a smooth muscle cell lineage.

MATERIALS AND METHODS

Polymer Synthesis and Characterization

PEGDA was prepared as previously described [41] by combining 0.1 mmol/ml dry PEG (3.4, 6.0, or 10.0 kDa; Fluka), 0.4 mmol/ml acryloyl chloride, and 0.2 mmol/ml triethylamine in anhydrous dichloromethane and stirring under argon overnight. The resulting solution was washed with 2 M K_2CO_3 and separated into aqueous and dichloromethane phases to remove HCl. The organic phase was subsequently dried with anhydrous $MgSO_4$, and PEGDA was precipitated in diethyl ether, filtered, and dried under vacuum. Acrylation of the PEG end hydroxyl groups was characterized by ^{1}H-NMR to be ≈ 95%.

IPN Fabrication Process

Collagen-PEGDA IPNs were fabricated under sterile conditions via a three-step process outlined schematically in Figure 1: 1) the physical crosslinking of a pure collagen network, 2) followed by the infiltration of the collagen hydrogel with a 3.4 kDa, 6.0 kDa or 10.0 kDa PEGDA solution, and 3) UV polymerization of the infiltrating PEGDA solution. In brief,

ice-cold high-concentration rat tail collagen I (BD Biosciences) was diluted and neutralized with 1 M NaOH, 10X PBS and dIH_2O to achieve the desired final collagen concentration (1.5 mg/mL, 3 mg/ml, or 5 mg/mL) in 1X PBS. Three hundred microliters of the neutralized ice-cold solution was then pipetted into BD Falcon culture inserts (12 mm diameter, 0.8 μm pore size) followed by polymerization via 30 min incubation at 37 °C and 5% CO_2. The resulting hydrogels were then immersed for 30 min in serum-free medium (SFM) composed of phenol-red free, high glucose DMEM (Gibco, Life Technologies) supplemented with 1% sodium pyruvate (Gibco, Life Technologies) and 1% Glutamax (Gibco, Life Technologies).

The second polymer network was created as follows: the SFM solution surrounding the previously cured collagen constructs was carefully removed and replaced with 1.7 ml of sterile-filtered SFM containing 11.7% w/v PEGDA and 0.26% w/v photoinitiator (Irgacure 2959). The concentration of PEGDA in this precursor solution was selected to achieve a nominal PEGDA concentration of approximately 10% w/v PEGDA within the collagen hydrogel. This PEGDA solution was then allowed to infiltrate the collagen network for 15–60 min at 37 °C. Excess PEGDA solution was then removed, and the PEGDA within the collagen hydrogel was polymerized by 6 min exposure to longwave UV light (Spectroline, ≈ 6 mW/cm^2, 365 nm). The resulting IPNs were immersed in culture media (CM; SFM supplemented with 10% MSC qualified FBS) until further analysis.

Tailoring Infiltration Time—The fabrication of stable and homogeneous IPNs by the above methodology requires that the infiltration time of the PEGDA solution be appropriately selected. To determine the penetration time necessary for the infiltrating PEGDA solution to reach its equilibrium concentration within the collagen hydrogel, an 11.7% w/v solution of an intermediate molecular weight PEGDA (6.0 kDa) was allowed to diffuse into a 3.0 mg/mL collagen hydrogel for 15 min, 30 min, 45 min or 60 min at 37 °C prior to UV polymerization. The resulting IPNs were immersed in CM for 24 h, after which they were exposed to the mechanical and swelling assessments described below. Pure collagen (3 mg/mL) and pure PEGDA (6 kDa, 10% w/v) hydrogel controls were also evaluated by the same methods.

Rheological Testing: Three to six hydrogel discs (8 mm diameter) per PEGDA infiltration time were used to characterize the rheological behavior of each resulting IPN. Hydrogels were blotted gently to remove excess water and placed on the testing stage of an Anton-Paar Physica MCR 301 rheometer fitted with an 8 mm diameter upper platen. The gap distance between the upper and lower platen was adjusted to achieve a 100 μm indentation depth within each IPN. Dynamic oscillatory frequency sweeps were then conducted at room temperature between 0.1 Hz and 100 Hz, with 10 measurement points per decade at a constant shear stress of 2%. Shear storage modulus (G') and shear loss modulus (G'') were each evaluated as a function of frequency.

Tensile Ring Testing: The effect of infiltration time on IPN mechanical properties was also evaluated using a modification of the circumferential property testing technique previously validated for arterial ring specimens [42]. In brief, three to five 8 mm discs were further separated into a 6 mm inner disc and an outer 8 mm ring using a 6 mm sterile biopsy punch. Each outer 8 mm ring was mounted onto an Instron 3342 by threading opposing stainless

steel hooks through the segment lumen. The hooks were then uniaxially separated at a rate of 6 mm/min until construct failure. As hook separation increased, the mounted ring was drawn into an increasingly oblong conformation. Johnson *et al.* confirmed that the force applied by the hooks to this oblong oval could be approximated as being equally distributed between two rectangles, each with sides equal to the width and wall thickness, h_v, of the ring. The gauge length, l_g, was taken to be the inner diameter, D_v, of the unstretched ring plus h_v, and the elastic modulus, E, of each sample was defined as the slope of the resulting linear stress–strain curve.

Swelling: Swelling measurements were performed as an additional indicator of the degree of PEGDA infiltration within the collagen networks. Twenty-four hours following IPN fabrication, three to six swollen constructs per IPN type were transferred to sterile PBS for 4 h at room temperature, after which the swollen weight (W_s) of each sample was recorded. The dry weight (W_d) of each specimen was subsequently recorded after 24 h of lyophilization. The equilibrium mass swelling ratio (q) was then calculated for each collagen-PEGDA IPN formulation as $q=\frac{W_s}{W_d}$.

Based on the resulting rheological and swelling data, it was determined that 45 min was sufficient for equilibrium PEGDA infiltration to be achieved in the collagen networks employed (Figure 2). However, to ensure equilibrium PEGDA infiltration, all further collagen-PEGDA IPNs were prepared using a 60 min infiltration time.

Tailoring the Mechanical Properties of Collagen-PEGDA IPNs

Varying the Molecular Weight of PEGDA: In pure PEGDA hydrogels, scaffold mechanical properties can be modulated by varying PEGDA molecular weight (MW) and/or concentration [37, 38, 43]. In this study, we chose to focus on the effects of PEGDA MW in modulating IPN mechanical properties. We did not vary PEGDA concentration, as increasing PEGDA concentration would have extended the time needed for the infiltrating PEGDA solution to achieve equilibrium within the collagen hydrogel. In examining the effects of PEGDA MW, the concentration of collagen within the collagen hydrogel was maintained at 3 mg/mL and the PEGDA MW in the infiltration solution was varied (3.4 kDa, 6.0 kDa, or 10.0 kDa PEGDA) with a 60 min infiltration time. The resulting IPNs and corresponding pure PEGDA and collagen hydrogel controls were immersed in CM for 24 h, followed by ring tensile testing as described above.

Varying the Concentration of Collagen: By varying the concentration of collagen in the hydrogel precursor solution, the stiffness of collagen hydrogels can be tuned. We therefore also examined the potential impact of variations in collagen concentration on overall IPN tensile properties. In brief, collagen hydrogels were prepared at 1.5 mg/mL, 3 mg/mL, and 5 mg/mL. An 11.7% w/v solution of the intermediate molecular weight PEGDA (6.0 kDa) was allowed to infiltrate the collagen gels for 60 min, followed by UV polymerization. After 24 h immersion in CM, mechanical testing was performed according to the rheological testing method described above.

IPN Microarchitectural Characterization

For microstructural assessment, 8 mm diameter collagen-PEGDA IPN discs were fabricated as described above using 3 mg/mL of collagen and 6.0 kDa PEGDA. Following 24 h immersion in CM, the IPN discs were processed for confocal microscopy or scanning electron microscopy (SEM), as outlined below.

Confocal Microscopy Imaging—The collagen-PEGDA IPN discs were fixed in formalin for 1 h, and 1 mm thick transverse sections were cut from each disc using a razor blade. Each section was washed with PBS and blocked with 3% bovine serum albumin (BSA) in PBS for 1 h. Samples were then exposed to primary antibody for collagen I (Rockland Immunochemicals) diluted in staining buffer (PBS containing 3% BSA and 0.05% Tween 20) for 12 h at 4 °C. Sections were subsequently rinsed 3 times with PBS, and donkey anti-rabbit Alexa Fluor 488 secondary antibody (Life Technologies) diluted in staining buffer was applied for 12 h at 4 °C. Following rinsing in PBS to remove unbound secondary antibody, confocal microscopy was performed using a Zeiss LSM 510 META confocal microscope equipped with a 40X water immersion objective. Four randomly selected regions in each sample segment were imaged.

Scanning Electron Microscopy Imaging—SEM was performed on collagen-PEGDA IPN hydrogels using a FEI Quanta 600F SEM with secondary electron detector. The hydrogels were prepared for electron microscopy by transverse sectioning, followed by fixation and serial dehydration with ethanol and hexamethyldisilazane according to the method described by Raub *et al.* [44]. Prior to imaging, dried hydrogels were mounted on SEM sample stages using carbon tape and sputter coated with Pd/Pt to a thickness of 6 nm using a Cressington 208HR sputter coater. Each specimen was then imaged at 5 kV using magnifications of 1500X and 40000X.

Cell Studies

Cryopreserved human mesenchymal stem cells (MSCs; Lonza) at passage 2 were thawed and expanded in monolayer culture. Prior to encapsulation, cells were maintained at 37 °C and 5% CO_2 in MesenPRO RS medium (Gibco, Life Technologies). For each of the cell studies below, MSCs were harvested at passage 4 and encapsulated at 7.5×10^5 cells/ml as described above. Collagen-PEGDA IPNs containing 3 mg/mL collagen and 6.0 kDa PEGDA were selected for evaluation due to the prior use of 10 % w/v 6.0 kDa PEGDA hydrogels in vascular tissue engineering studies [45, 46]. Cells were allowed to spread in the collagen network for 0 h, 4 h or 6 h in either SFM or CM prior to infiltration with an 11.7% w/v 6.0 kDa PEGDA solution for 60 min, followed by 6 min exposure to longwave UV light. The resulting cell-laden IPNs were incubated at 37 °C and 5% CO_2 and cultured in CM for up to 14 days with media changes every 2 days.

Cell Viability Assessments—Twenty-four hours post-fabrication, cell-laden IPNs were exposed to Live/Dead Cell Viability Assay reagents (Life Technologies) per the manufacturer's protocol. One mm thick transverse sections were cut from each hydrogel disc using a razor blade. Fluorescence images of the Live/Dead stained cells were obtained from 10 randomly selected regions of each transverse section using confocal microscopy.

Images were processed using ImageJ software to compute the number of viable versus dead cells.

Evaluation of the Ability of the IPN to Support Cell Elongation—To quantitatively assess cell elongation as a function of the time delay between collagen I network formation and PEGDA infiltration, cell-laden IPNs formed with delay times of 0, 4, and 6 h were fixed in formalin for 30 min, followed by exposure to 66 nM rhodamine phalloidin (Life Technologies) and 300 nM DAPI dilactate (Life Technologies) for 1 h at room temperature. Discs were then rinsed to remove unbound phalloidin and DAPI. One mm thick transverse sections were cut from each hydrogel disc using a razor blade. Cell shape information was then obtained from confocal microscopy images of the actin networks of the encapsulated cells from 4 randomly selected regions of each transverse section. Circularity (C) and roundness (R) measurements were obtained using ImageJ software. In brief, $\mathrm{C}=\frac{4*\pi*A}{P^2}$ and $\mathrm{R}=\frac{4*A}{\pi*a^2}$ were calculated for each cell, where *A* and *P* are the cell area and perimeter, respectively, and where *a* is the length of the major axis of the cell [47].

Assessment of Cell-Mediated IPN Compaction—Collagen-PEGDA IPNs were prepared with a 6 h time delay between collagen hydrogel formation and PEGDA infiltration to ensure MSC elongation. These IPNs were cultured for 14 days alongside pure PEGDA and pure collagen I hydrogel controls prepared with similar initial cell densities (7.5×10^5 cells/mL). Compaction was assessed by monitoring changes in hydrogel dimensions using a digital micrometer over the course of 14 days of culture.

Capacity of the IPN to Support Initial Smooth Muscle Cell Lineage Progression—Collagen-PEGDA IPNs were prepared with a 6 h time delay between collagen hydrogel formation and PEGDA infiltration to ensure MSC elongation. The resulting IPNs were initially immersed in DMEM containing 10% MSC-qualified FBS and 1% penicillin/streptomycin/amphotericin solution. After 24 h of culture, a set of gels was harvested as “day 0” specimens, snap-frozen, and stored at −80 °C until analysis. Remaining gels were then cultured in DMEM supplemented with 10% MSC-qualified FBS, and 10 ng/mL TGF-β_3, with media changes every two days. After 14 days of culture, these IPNs were harvested and snap-frozen for subsequent analysis.

MSC phenotypic progression within the day 14 IPNs was evaluated by qRT-PCR relative to day zero. Specifically, gene expression for smooth muscle alpha actin (SM-α-actin), smooth muscle 22 alpha (SM22α) and calponin h1 (CNN1) was quantified relative to the housekeeping gene GAPDH. Since TGF-β_3 can also induce chondrogenesis in MSC cultures [48], the chondrogenic markers sox9 and collagen II were also evaluated to assess the presence of this undesired lineage. In brief, mRNA was extracted using the Dynabeads mRNA direct kit (Ambion, Life Technologies). In brief, a 6 mm disc was cored from each of the IPN constructs and transferred to a 1.7 ml RNase-free conical tube containing 330 μL of the provided lysis binding buffer. The samples were then homogenized using a plastic RNase-free pestle (Kimble Chase) and incubated at room temperature for 10 min. Following incubation, the samples were centrifuged for 5 min at 10,000 rpm and the polyA-mRNA in the supernatant was harvested using 20 μL of Dynabeads oligo $(dT)_{25}$ magnetic beads.

Following rinsing steps, the polyA-mRNA was released from the Dynabeads in 100 μL of 10 mM Tris-HCl by heating the beads to 80 °C for 2 min.

Proprietary qRT-PCR verified primers for human SM-α-actin, SM22α, CNN1, sox9, collagen II and GAPDH were purchased from Origene. qRT-PCR was performed on each sample using a StepOne real-time PCR system (Life Technologies) and the SuperScript III Platinum One-Step qRT-PCR kit (Invitrogen, Life Technologies). mRNA levels for each gene of interest were assessed in duplicate for each construct. Approximately 3 ng of polyA-mRNA and 5 μL of 1 mM primer were added per 25 μL of reaction mixture. Amplification during the PCR phase was monitored by measuring the change in SYBR Green fluorescence, with ROX dye serving as a passive reference. A threshold fluorescence value at which each sample was in the exponential phase of amplification was identified using StepOne software v2.0. The amplification cycle at which a given sample exceeded this threshold was recorded as the C_t for that sample. For each sample, expression of each gene of interest was calculated relative to GAPDH using the $\Delta\Delta C_t$ method. Melting temperature analysis was performed for each PCR reaction to verify the appropriate amplification product.

Platelet Adhesion Assessment

The thrombogenicity of the collagen-PEGDA IPNs was evaluated relative to pure collagen hydrogels using platelet adhesion studies per standard protocols [49]. IPNs were fabricated using 3 mg/mL of collagen and 11.7 % w/v 6.0 kDa PEGDA via the sequential process described above. The resulting IPNs and corresponding collagen hydrogel controls were immersed in CM for 24 h, followed by exposure of four hydrogels from each group to 1 mL of porcine whole blood containing heparin (Lampire, Biological Laboratories). After 2 h of incubation, the blood was gently removed from each surface, and hydrogels were rinsed five times for 5 min at room temperature with 1 mL of Dulbecco's PBS (Gibco, Live Technologies). Adherent platelets were then lysed for 20 min at room temperature using 1 ml of lysis solution from the LDH Cytotoxicity Detection Kit (Roche). The total number of adhered cells was indirectly quantified by the measurement of lactate dehydrogenase (LDH) levels in the lysate [49].

Statistical Analyses

Data are reported as mean ± standard deviation. Comparison of sample means was performed using ANOVA followed by Tukey's post-hoc test (SPSS software), $p < 0.05$.

RESULTS

Tailoring the IPN Fabrication Process

In terms of fabricating the collagen-PEGDA IPNs, it was important to first identify the infiltration time needed for the infusing PEGDA precursor solution to reach its equilibrium concentration throughout the pre-formed collagen hydrogel [50]. Thus, a series of experiments were conducted in which the PEGDA infiltration solution was allowed to diffuse into a 3 mg/mL collagen hydrogel for 15 min, 30 min, 45 min or 60 min prior to UV-initiated PEGDA polymerization. The resulting IPNs were immersed in culture media for 24

h, after which they were characterized in terms of shear storage modulus (G′), shear loss modulus (G″), and mass swelling ratio (q). Results from these assays are shown in Figure 2A–C. As expected, both the G′ and G″ of the collagen-PEGDA IPNs increased with increasing infiltration time up through 45 min. Beyond this infiltration time, no further statistically significant changes in G′ or G″ were observed, indicating that equilibrium infusion of the PEGDA solution was achieved at 45 min infiltration time. Tensile ring testing supported these rheological results. Specifically, IPN tensile modulus increased from ≈ 37 kPa at a 15 min infiltration time to ≈ 78 kPa at a 45 min infiltration time (Table 1). Similarly, no further significant changes in IPN tensile modulus were observed between 45 min and 60 min infiltration time. These trends were also observed for tensile strength (Table 1).

As with mechanical property testing, mass swelling assessments can give quantitative insight into the extent of PEGDA diffusion into the collagen hydrogel prior to PEGDA crosslinking. The equilibrium mass swelling ratios of the collagen-PEGDA IPNs decreased with increasing infiltration time through 45 min ($p < 0.010$), after which no further significant reductions were observed (Figure 2C). Furthermore, the post-swelling concentration of PEGDA in IPNs as a function of infusion time was calculated from the obtained swelling data. The concentration of PEGDA in the IPN after 15 min of infiltration time reached 6.1 ± 0.1% w/v and monotonically increased until attaining equilibrium at 45 min infusion time. The equilibrium infusion time was set as the time beyond which the post-swelling PEGDA concentration in the IPN was statistically indistinguishable from that of the PEGDA control formulation (7.0% w/v post-swelling, 10% w/v nominal). Detailed data information of the post-swelling concentration of PEGDA in each IPN formulation as a function of infusion time has been reported in the Supplementary Table 1. As such, both the mechanical testing and swelling data indicate that a 45 min infiltration time was sufficient for an 11.7 % w/v solution of 6.0 kDa PEGDA to reach equilibrium levels within a 3 mg/mL collagen hydrogel. However, to ensure that equilibrium PEGDA infiltration was achieved in our studies, all further collagen-PEGDA IPNs were prepared using a 60 min infiltration time.

Mechanical Testing Assessment at Equilibrium PEGDA Infiltration

In further examining the mechanical data in Figure 2, the shear storage modulus (G′) and shear loss modulus (G″) were each substantially greater for the equilibrium IPN (45–60 min infiltration time) than for the single network PEGDA and collagen hydrogel controls. Specifically, the G′ for the IPN at 60 min infiltration time was 136-fold greater than the pure collagen control and 3-fold greater than the PEGDA control ($p < 0.001$). Similarly, a 140-fold increase in G″ was observed for the equilibrium IPN relative to the pure collagen hydrogel control ($p < 0.001$) and a 1.6-fold increase was observed relative to the PEGDA control ($p < 0.001$).

This increase in IPN storage and loss modulus relative to the individual component networks was also reflected in the tensile modulus data. Specifically, the tensile modulus of the collagen-PEGDA IPN at equilibrium PEGDA infiltration was approximately 2.5-fold greater than that of the pure PEGDA control ($p = 0.001$, Table 1). Similarly, the tensile strength (TS) of the IPN at 60 min infiltration time was ≈ 2.4-fold greater than the TS of the PEGDA control ($p = 0.002$), with a TS of approximately 100 kPa being achieved for the collagen-

PEGDA IPN (Table 1). This value of TS is over an order of magnitude larger than that of the tubular collagen hydrogels previously utilized in vascular graft construction [5].

To gain insight into the elasticity of the collagen-PEGDA IPN, the rheological data was used to determine the loss tangent (G''/G') of the IPN compared to that of the pure PEGDA control. The loss tangent for the collagen-PEGDA IPN was 0.11 ± 0.01, significantly lower than the 0.19 ± 0.06 loss tangent of pure PEGDA hydrogels ($p = 0.040$). This indicates that the IPNs may have increased elasticity relative to pure PEGDA gels, which are generally considered to be highly elastic.

Post-Encapsulation Cell Viability

Prolonged exposure of cells to high concentrations of solubilized, uncrosslinked PEGDA can have cytotoxic effects. As such, it was important to assess the viability of cells through the sequential encapsulation process associated with IPN formation. Toward this end, human MSCs were encapsulated within a 3 mg/mL collagen hydrogel followed by either a 0 h or a 6 h delay time. The gels were then exposed to an 11.7 % w/v solution of 6.0 kDa PEGDA for 60 min prior to UV polymerization. Live/Dead staining performed 24 h following encapsulation indicated cell viability levels of 91.1 ± 1.2% in IPNs fabricated with 0 h delay-time between collagen network formation and the onset of PEGDA infiltration. IPNs formed with a 6 h delay-time were associated with a cell viability of 95.1 ± 1.6%. Representative Live/Dead images can be seen in Supplementary Figure 1. These viability results are consistent with data from Nuttelman *et al.*, which showed human MSC viability in photocrosslinked PEGDA hydrogels to fall between 75% and 97% [51]. In addition, the present MSC viability results suggest that the IPN fabrication strategy used in this study provides similar cytocompatibility compared to other IPN cell encapsulation strategies, where viability ranges from 47 % to 96 % [52, 53]. Thus, a 60 min exposure to solubilized PEGDA prior to crosslinking appears to be cytocompatible at the concentration of PEGDA employed.

Tailoring the Mechanical Properties of Collagen-PEGDA IPNs

In pure PEGDA hydrogels, scaffold mechanical properties can be modulated by varying PEGDA molecular weight (MW) and concentration [37, 38, 54, 55]. Collagen hydrogel mechanical properties can also be tuned by tailoring the concentration of collagen [14]. To demonstrate the tunability of this IPN system, we have therefore examined the effects of PEGDA MW and collagen concentration on IPN mechanical properties.

Effect of PEGDA MW—In assessing the effects of PEGDA MW, 3.4 kDa, 6 kDa, and 10 kDa PEGDA was utilized. Consistent with PEGDA hydrogel literature, a decrease in PEGDA MW led to a significant increase in tensile modulus for the pure PEGDA controls ($p = 0.008$; Figure 3A). This modulation of stiffness by PEGDA MW was also reflected in the collagen-PEGDA IPN series, with the average tensile modulus of the IPNs increasing from 25.2 ± 1.4 kPa for 10.0 kDa PEGDA to 103.2 ± 20.3 kPa for 3.4 kDa PEGDA ($p \leq 0.001$). Rheological assessments indicated a similar increase in IPN shear elastic modulus with decreasing PEGDA MW ($p < 0.028$), with G' for the IPN containing 3.4 kDa PEGDA being ≈ 2.2-fold greater than for the IPN containing 10 kDa PEGDA (Table 2). TS of the collagen-

PEGDA IPNs also increased from ≈ 47 kPa to over 100 kPa as PEGDA MW decreased from 10 kDa to 3.4 kDa ($p = 0.002$, Figure 3B).

These PEGDA MW data also reveal consistent trends with the equilibrium IPN results containing 6.0 kDa PEGDA discussed in the previous section. Specifically, the average tensile modulus ($p \leq 0.001$) and average TS ($p \leq 0.002$) of the IPNs containing 3.4 kDa, 6.0 kDa, or 10 kDa PEGDA was increased 1.6–2.5-fold relative to the corresponding pure PEGDA controls. Furthermore, the elasticity of the IPNs was greater than their corresponding pure PEGDA counterparts per loss tangent calculations for each PEGDA MW examined (Table 2). Importantly, several of the examined IPN tensile modulus values fall within the range of health vascular tissue (40 – 900 kPa) [16, 17].

Effect of Collagen Concentration—To assess the effect of collagen concentration on IPN mechanical properties, 3 collagen hydrogel types were prepared: 1.5 mg/mL, 3 mg/mL, and 5 mg/mL. These hydrogels were then exposed to an 11.7 % w/v solution of 6.0 kDa PEGDA for 60 min, followed by PEGDA polymerization. The average rheological properties of the resulting IPNs are given in Table 3. As anticipated, G' increased with increasing collagen concentration, from 11.0 ± 4.6 kPa at 1.5 mg/mL collagen to 21.7 ± 4.1 kPa at 5.0 mg/mL collagen ($p = 0.003$). Furthermore, the loss tangent decreased by a factor of 2 from 1.5 mg/mL collagen to 5 mg/mL collagen, indicating that IPN elasticity increased with increasing collagen concentration ($p = 0.001$). These results are consistent with the increased G' and increased elasticity reported for pure collagen gels over a similar collagen concentration range [56]. Cumulatively, the above PEGDA MW and collagen concentration data demonstrate the mechanical tunability of the collagen-PEGDA IPNs.

IPN Microarchitectural Characterization

To further characterize the developed IPNs, their microarchitecture was examined using standard microscopy techniques To visualize the native state and distribution of the fibrillar collagen network within the swollen hydrogels, immunostaining for collagen I was performed followed by confocal microscopy. Representative confocal images of a 3 mg/mL collagen hydrogel, 6.0 kDa PEGDA 10% w/v hydrogel and the 60 min infiltrated IPN with 6.0 kDa PEGDA are shown in Figure 4. The fibrillar collagen network within the pure collagen and the IPN is apparent, and the collagen fibrils appear to be relatively evenly distributed within the matrix. In contrast, no fibers were observed in the pure PEGDA control formulation, which has no intrinsic fluorescence.

To visualize both the PEGDA and collagen components of the IPN, SEM imaging was employed. Figure 5A shows representative SEM images of a pure PEGDA hydrogel, whereas Figure 5B displays representative images of a collagen-PEGDA IPN. In the IPN images, collagen fibrils entangled with flat PEGDA structures can be seen. The average thickness of these collagen fibrils was measured as approximately 60 nm using the SEM software measurement tool. This diameter value is consistent with that observed in other studies for collagen hydrogels cured at neutral pH and temperature of 37 °C [44].

IPN Ability to Support an Elongated Cell Phenotype

Pure PEGDA hydrogels are not permissive to cell elongation following PEGDA polymerization, even in the presence of incorporated cell adhesion ligands. This is due to the tight, nanoscale mesh structure and resistance to degradation that is characteristic of PEGDA gels [57]. To enable cell elongation within this IPN system, we therefore chose to rely on the capacity of collagen hydrogels to facilitate cell spreading. In brief, MSCs were encapsulated within 3 mg/mL collagen hydrogels, and then incubated in the presence of serum-free culture medium for 0, 4, or 6 h prior to exposure to PEGDA (also dissolved in serum free medium) for 60 min. Following PEGDA polymerization, each disc was immersed in medium containing 10% serum and cultured for 24 h prior to imaging.

The average extent of cell elongation was assessed by quantification of cell circularity (C) and roundness (R). The measures serve as quantitative measures of cell shape, where values of C and R significantly less than 1 correspond to a high degree of cell elongation and values of C and R closer to 1 correspond to more rounded morphology. As expected, both cell circularity and roundness decreased as the time for cell spreading in the collagen network prior to PEGDA infusion increased from 0 h to 6 h. Specifically, circularity decreased from 0.5 to 0.28 as the delay-time between collagen network formation and PEGDA infiltration increased from 0 h to 6 h ($p < 0.001$, Figure 6A). Similarly, roundness was reduced from 0.64 to 0.38 with increasing delay-time ($p < 0.001$, Figure 6B). These quantitative changes in cell morphology corresponded to a shift from rounded cells at 0 h to spindle-shaped cells at 6 h, as shown in Figure 7. These cell shapes were maintained through 2 weeks of culture (Supplementary Figure 2).

Cumulatively, the present data demonstrate that the sequentially polymerized collagen-PEGDA hydrogel system retains the benefits of collagen hydrogels in terms of enabling cell elongation.

IPN Resistance to Cell-Mediated Compaction

To assess the resistance of the collagen-PEGDA IPNs to cell-mediated compaction, IPNs fabricated with a 6 h delay time, i.e. containing elongated MSCs, were cultured for 14 days. Compaction was assessed by monitoring changes in hydrogel dimensions over the course of 14 days of culture. No alteration in IPN thickness was observed through the culture period (Figure 8A). Similarly, the lateral dimensions of the IPN networks were also maintained over 14 days of culture (Figure 8B **and the** Supplementary Table 2). These results are consistent with the resistance to cell-mediated compaction characteristic of pure PEGDA hydrogels. In contrast, the diameter of pure collagen hydrogels at 14 days of culture was reduced 60.3 ± 8.2 % relative to day 0 (Figure 8B).

Collagen hydrogels enable significant cell proliferation, whereas PEGDA-containing hydrogels do not, due in part to their nanoscale crosslinks and slow degradation rates [37, 38]. Thus, the above studies do not enable matrix compaction resulting from a potential increase in cell number to be distinguished from intrinsic hydrogel susceptibility to compaction. An additional set of hydrogels were therefore prepared containing h-MSCs pre-treated with 8 μg/mL mitomycin C (MMC), a potent inhibitor of cell proliferation. MMC

pre-treated hydrogels could be considered to have a relatively constant total cell number over the 14 day culture period. In the MMC-treated set, differences in the extent of collagen hydrogel and IPN compaction could therefore be attributed to differences in their intrinsic susceptibility to cell-mediated compaction. Significant reduction in the diameter (~37.9 ± 3.2 %) of the MMC-treated collagen hydrogels was observed, although no change was observed for the IPNs (Figure 8B). Therefore, the collagen-PEGDA IPNs displayed an increased resistance to cell-mediated matrix compaction relative to pure collagen.

IPN Capacity to Support Smooth Muscle Cell Lineage Progression

Adult mesenchymal stem cells (MSCs) are increasingly used as a source of smooth muscle cells for tissue engineered vascular grafts [6–10]. We therefore evaluated the capacity of the collagen-PEGDA IPNs to support MSC differentiation to vascular smooth muscle cells in the presence of TGF-β_3, a growth factor which can support either smooth muscle cell or chondrogenic differentiation depending on microenvironmental factors [58].

Following 14 days of culture, elongated MSCs encapsulated within an IPN containing 3 mg/mL collagen and 10 % w/v of 6.0 kDa PEGDA exhibited a 13.7-, 9.8-, and 9.5-fold increase in the gene expression of smooth muscle cells markers SMα-actin, SM22α and CNN1, respectively, relative to day zero ($p < 0.004$, Figure 9). On the other hand, no alteration in gene expression of the chondrogenic transcription factor sox9 was observed between day 14 and day 0 of culture, and mRNA for collagen II was not detected. These data indicate that the 6.0 kDa PEGDA IPN formulation was able to support the initial stages of MSC smooth muscle cell lineage progression in the presence of elongated cells.

Initial Assessment of IPN Thrombogenicity

As an initial thrombogenicity assessment, collagen-PEGDA IPNs were exposed to porcine whole blood under static conditions and the levels of platelet adhesion and clot formation were assessed relative to collagen hydrogel positive controls. The degree of platelet adhesion supported by the IPNs was ≈ 40% lower than that supported by the collagen controls ($p = 0.001$, Figure 10A) and clot formation was qualitatively reduced (Figure 10B). Thus, the presence of PEGDA within the IPNs appeared to enhance their thromboresistance relative to pure collagen hydrogels.

DISCUSSION

The aim of the present work has been to develop an IPN which would retain the benefits of collagen in terms of enabling robust cell elongation, but which would display enhanced mechanical stiffness and strength, improved thromboresistance, and high resistance to compaction. To allow for cell elongation within the IPN networks despite the presence of PEGDA, a delay time was introduced between the formation of the cell-laden collagen network and subsequent infiltration with PEGDA. This is in contrast to most IPNs, including those previously formed from PEG and collagen [39], which are generally prepared by mixing the two component polymers followed by their simultaneous crosslinking into interwoven networks [25, 27, 28, 39]. In the present work, we have demonstrated that collagen-PEGDA IPNs fabricated by this sequential polymerization process permit control

over the degree of cell elongation, from rounded at a 0 h delay time to increasingly elongated at a 6 h delay-time. MSC viability through the sequential polymerization process was > 90%, irrespective of delay time. Furthermore, elongated MSCs within a ≈ 60 kPa collagen-PEGDA IPN progressed through the initial stages of smooth muscle cell differentiation when cultured in the presence of TGF-β_3, a growth factor that can stimulate either chondrogenesis or smooth muscle cell formation depending on the local cell environment.

In terms of mechanical properties, the observed improvement in rheological and tensile moduli in the collagen-PEGDA IPNs relative to their single network counterparts is in agreement with previous studies that used PEG [50] or poly (2-hydroxyethyl methacrylate) (HEMA)-based IPN systems [59]. The synergistic increase in TS observed in the collagen-PEGDA IPN relative to the additive TS of the component networks is also consistent with existing IPN literature [27, 28]. Furthermore, the elasticity of the IPNs was greater than their corresponding pure PEGDA counterparts, per loss tangent calculations. Given the importance of biomaterial resistance to dilation in vascular graft applications, the ability to modulate scaffold elasticity is advantageous in graft design.

Also, consistent with existing literature is the tunability of collagen-PEGDA IPN mechanical properties in response to changes in PEGDA MW and collagen concentration. It is anticipated that tailoring the PEGDA concentration in the infiltration solution would result in a further broadening of achievable tensile and rheological properties [38, 60, 61], although longer infiltration times may be needed for more concentrated PEGDA solutions to reach equilibrium within the collagen hydrogel.

Collagen-PEGDA IPNs containing elongated MSCs also exhibited a high degree of physical stability, with construct dimensions being maintained over 14 days of culture with no evidence of significant cell-mediated compaction. This is important for vascular graft applications, where control over graft dimensions and stability is critical. Moreover, the collagen-PEGDA IPNs displayed significantly reduced platelet adhesion and clot formation relative to pure collagen hydrogels. Both the increased physical stability and increased thromboresistance of the collagen-PEGDA IPNs relative to pure collagen hydrogels result from the physical properties of PEGDA hydrogels. Specifically, the nanoscale crosslink density and resistance to degradation characteristic of pure PEGDA networks limit cell-mediated network compaction [57]. In addition, the non-fouling or passivating nature of PEGDA is considered to underlie its thromboresistance [29, 30].

This sequential polymerization/time-delay approach to creating hybrid natural-synthetic IPNs containing elongated cells is not limited to collagen and PEGDA. For instance, fibrinogen-based hydrogels could potentially be employed in place of collagen. Furthermore, the fabrication of collagen-PEGDA IPNs with directionally aligned collagen fibers could be achieved if the protein fibers are aligned prior to PEGDA infiltration and polymerization via the application of mechanical strain or a magnetic field [3].

CONCLUSIONS

In the present work, a collagen-PEGDA IPN has been developed which retains many of the benefits of pure collagen hydrogels but which displays improved stiffness, strength, physical stability, and blood compatibility. The introduction of a variable time delay between the formation of the collagen hydrogel and the formation of the secondary PEGDA network enables tight control over cell spreading, ensuring the robust cell elongation needed for vascular graft applications despite the present of PEGDA. This ability to control the degree of cell spreading combined with the broad tunability of the collagen-PEGDA IPN modulus and strength also opens the potential use of these scaffolds in a range of other tissue engineering applications.

Supplementary Material

Refer to Web version on PubMed Central for supplementary material.

Acknowledgments

We would like to acknowledge the NSF DMR CAREER Award 1346807, NIH R01 EB013297, and the NIH R03 EB0152167 for funding. We would also like to thank Dr. Ryan Gilbert at RPI for use of his Anton-Paar Physica MCR 301 rheometer and Mr. Tom Stephens from the Microscopy and Imaging Center at Texas A&M University for expert assistance during SEM imaging.

References

1. Latimer CA, Nelson M, Moore CM, Martin KE. Effect of collagen and elastin content on the burst pressure of human blood vessel seals formed with a bipolar tissue sealing system. J Surg Res. 2014; 186(1):73–80. [PubMed: 24035229]
2. L'Heureux N, Germain L, Labbé R, Auger FA. In vitro construction of a human blood vessel from cultured vascular cells: A morphologic study. J Vas Surg. 1993; 17(3):499–509.
3. Tranquillo RT, Girton TS, Bromberek BA, Triebes TG, Mooradian DL. Magnetically orientated tissue-equivalent tubes: application to a circumferentially orientated media-equivalent. Biomaterials. 1996; 17(3):349–57. [PubMed: 8745332]
4. Weinberg C, Bell E. A blood vessel model constructed from collagen and cultured vascular cells. Science. 1986; 231(4736):397–400. [PubMed: 2934816]
5. Weinberg CB, Bell E. A blood vessel model constructed from collagen and cultured vascular cells. Science. 1986; 231:397–400. [PubMed: 2934816]
6. Gong Z, Calkins G, Cheng E-c, Krause D, Niklason LE. Influence of culture medium on smooth muscle cell differentiation from human bone marrow derived mesenchymal stem cells. Tissue Eng Part A. 2009; 15(2):319–30. [PubMed: 19115826]
7. Gong Z, Niklason LE. Small-diameter human vessel wall engineered from bone marrow-derived mesenchymal stem cells (hMSCs). FASEB J. 2008; 22:1635. [PubMed: 18199698]
8. Huang NF, Li S. Mesenchymal stem cells for vascular regeneration. Regen Med. 2008; 3(6):877–92. [PubMed: 18947310]
9. Gong Z, Niklason LE. Use of human mesenchymal stem cells as alternative source of smooth muscle cells in vessel engineering. Methods Mol Biol. 2011; 698:279–94. [PubMed: 21431526]
10. Kurpinski K, Lam H, Chu J, Wang A, Kim A, Tsay E, et al. Transforming growth factor-beta and notch signaling mediate stem cell differentiation into smooth muscle cells. Stem Cells. 2010; 28(4):734–42. [PubMed: 20146266]
11. Awad HA, Butler DL, Harris MT, Ibrahim RE, Wu Y, Young RG, et al. In vitro characterization of mesenchymal stem cell-seeded collagen scaffolds for tendon repair: effects of initial seeding density on contraction kinetics. J Biomed Mater Res. 2000; 51(2):233–40. [PubMed: 10825223]

12. Angele P, Abke J, Kujat R, Faltermeier H, Schumann D, Nerlich M, et al. Influence of different collagen species on physico-chemical properties of crosslinked collagen matrices. Biomaterials. 2004; 25(14):2831–41. [PubMed: 14962561]
13. Sosnik A, Sefton MV. Semi-synthetic collagen/poloxamine matrices for tissue engineering. Biomaterials. 2005; 26(35):7425–35. [PubMed: 16023714]
14. Yang YL, Kaufman LJ. Rheology and confocal reflectance microscopy as probes of mechanical properties and structure during collagen and collagen/hyaluronan self-assembly. Biophys J. 2009; 96(4):1566–85. [PubMed: 19217873]
15. Zuidema JM, Rivet CJ, Gilbert RJ, Morrison FA. A protocol for rheological characterization of hydrogels for tissue engineering strategies. J Biomed Mater Res B Appl Biomater B. 2013; 102(5): 1063–73.
16. Roeder R, Wolfe J, Lianakis N, Hinson T, Geddes LA, Obermiller J. Compliance, elastic modulus, and burst pressure of small-intestine submucosa (SIS), small-diameter vascular grafts. J Biomed Mater Res. 1999; 47(1):65–70. [PubMed: 10400882]
17. Blondel WCPM, Lehalle B, Maurice G, Wang X, Stoltz J-F. Rheological properties of fresh and cryopreserved human arteries tested in vitro. Rheol Acta. 2000; 39(5):461–8.
18. L'heureux N, Paquet S, Labbe R, Germain L, Auger FA. A completely biological tissue-engineered human blood vessel. FASEB J. 1998; 12(1):47–56. [PubMed: 9438410]
19. Geho DH, Smith WI, Liotta LA, Roberts DD. Fibronectin-based masking molecule blocks platelet adhesion. Bioconjugate Chem. 2003; 14(4):703–6.
20. Keuren JFW, Wielders SJH, Driessen A, Verhoeven M, Hendriks M, Lindhout T. Covalently-bound peparin makes collagen thromboresistant. Arterioscler Thromb Vasc Biol. 2004; 24(3):613–7. [PubMed: 14707039]
21. Girton TS, Oegema TR, Tranquillo RT. Exploiting glycation to stiffen and strengthen tissue equivalents for tissue engineering. J Biomed Mater Res. 1999; 46(1):87–92. [PubMed: 10357139]
22. Mott JD, Khalifah RG, Nagase H, Shield CF 3rd, Hudson JK, Hudson BG. Nonenzymatic glycation of type IV collagen and matrix metalloproteinase susceptibility. Kidney Int. 1997; 52(5): 1302–12. [PubMed: 9350653]
23. Rault I, Frei V, Herbage D, Abdul-Malak N, Huc A. Evaluation of different chemical methods for cros-linking collagen gel, films and sponges. J Mater Sci-Mater M. 1996; 7(4):215–21.
24. Golomb G, Schoen FJ, Smith MS, Linden J, Dixon M, Levy RJ. The role of glutaraldehyde-induced cross-links in calcification of bovine pericardium used in cardiac valve bioprostheses. Am J Pathol. 1987; 127(1):122–30. [PubMed: 3105321]
25. Banerjee S, Ray S, Maiti S, Sen KK, Bhattacharyya U, Kaity S, et al. Interpenetrating polymer network (IPN): a novel biomaterial. IJAP. 2010; 2:28–34.
26. Fei R, George JT, Park J, Means AK, Grunlan MA. Ultra-strong thermoresponsive double network hydrogels. Soft Matter. 2013; 9(10):2912–9.
27. Sun J-Y, Zhao X, Illeperuma WRK, Chaudhuri O, Oh KH, Mooney DJ, et al. Highly stretchable and tough hydrogels. Nature. 2012; 489(7414):133–6. [PubMed: 22955625]
28. Darnell MC, Sun J-Y, Mehta M, Johnson C, Arany PR, Suo Z, et al. Performance and biocompatibility of extremely tough alginate/polyacrylamide hydrogels. Biomaterials. 2013; 34(33):8042–8. [PubMed: 23896005]
29. Cosgriff-Hernandez E, Hahn MS, Russell B, Wilems T, Munoz-Pinto D, Browning MB, et al. Bioactive hydrogels based on designer collagens. Acta Biomater. 2010; 6(10):3969–77. [PubMed: 20466083]
30. West JL, Hubbell JA. Separation of the arterial wall from blood contact using hydrogel barriers reduces intimal thickening after balloon injury in the rat: The roles of medial and luminal factors in arterial healing. Proc Natl Acad Sci. 1996; 93(23):13188–93. [PubMed: 8917566]
31. Jimenez-Vergara AC, Munoz-Pinto DJ, Becerra-Bayona S, Wang B, Iacob A, Hahn MS. Influence of glycosaminoglycan identity on vocal fold fibroblast behavior. Acta Biomater. 2011; 7(11): 3964–72. [PubMed: 21740987]
32. Young JL, Engler AJ. Hydrogels with time-dependent material properties enhance cardiomyocyte differentiation in vitro. Biomaterials. 2011; 32(4):1002–9. [PubMed: 21071078]

33. Wang D, Hill DJT, Peng H, Symons A, Varanasi S, Whittaker AK, et al. Development of injectable biodegradable multi-arms PEG-based hydrogels: swelling and degradation investigations. Macromol Symp. 2010; 296(1):233–7.
34. Sokic S, Papavasiliou G. Controlled proteolytic cleavage site presentation in biomimetic PEGDA hydrogels enhances neovascularization in vitro. Tissue Eng Part A. 2012; 18(23–24):2477–86. [PubMed: 22725267]
35. Metters A, Hubbell J. Network formation and degradation behavior of hydrogels formed by Michael-type addition reactions. Biomacromolecules. 2005; 6(1):290–301. [PubMed: 15638532]
36. Rice MA, Sanchez-Adams J, Anseth KS. Exogenously triggered, enzymatic degradation of photopolymerized hydrogels with polycaprolactone subunits: experimental observation and modeling of mass loss behavior. Biomacromolecules. 2006; 7(6):1968–75. [PubMed: 16768421]
37. Lin S, Sangaj N, Razafiarison T, Zhang C, Varghese S. Influence of physical properties of biomaterials on cellular behavior. Pharm Res. 2011; 28(6):1422–30. [PubMed: 21331474]
38. Liao H, Munoz-Pinto D, Qu X, Hou Y, Grunlan MA, Hahn MS. Influence of hydrogel mechanical properties and mesh size on vocal fold fibroblast extracellular matrix production and phenotype. Acta Biomater. 2008; 4(5):1161–71. [PubMed: 18515199]
39. Chan BK, Wippich CC, Wu C-J, Sivasankar PM, Schmidt G. Robust and semi-interpenetrating hydrogels from poly(ethylene glycol) and collagen for elastomeric tissue scaffolds. Macromol Biosci. 2012; 12(11):1490–501. [PubMed: 23070957]
40. Kloxin AM, Kasko AM, Salinas CN, Anseth KS. Photodegradable hydrogels for dynamic tuning of physical and chemical properties. Science. 2009; 324(5923):59–63. [PubMed: 19342581]
41. Munoz-Pinto DJ, McMahon RE, Kanzelberger MA, Jimenez-Vergara AC, Grunlan MA, Hahn MS. Inorganic-organic hybrid scaffolds for osteochondral regeneration. J Biomed Mater Res A. 2010; 94(1):112–21. [PubMed: 20128006]
42. Johnson CP, How T, Scraggs M, West CR, Burns J. A biomechanical study of the human vertebral artery with implications for fatal arterial injury. Forensic Sci Int. 2000; 109(3):169–82. [PubMed: 10725653]
43. Waters DJ, Engberg K, Parke-Houben R, Hartmann L, Ta CN, Toney MF, et al. Morphology of photopolymerized end-linked poly(ethylene glycol) hydrogels by small-angle X-ray scattering. Macromolecules. 2010; 43(16):6861–70. [PubMed: 21403767]
44. Raub CB, Suresh V, Krasieva T, Lyubovitsky J, Mih JD, Putnam AJ, et al. Noninvasive assessment of collagen gel microstructure and mechanics using multiphoton microscopy. Biophys J. 2007; 92(6):2212–22. [PubMed: 17172303]
45. Jimenez-Vergara AC, Guiza-Arguello V, Becerra-Bayona S, Munoz-Pinto DJ, McMahon RE, Morales A, et al. Approach for fabricating tissue engineered vascular grafts with stable endothelialization. Ann Biomed Eng. 2010; 38(9):2885–95. [PubMed: 20464634]
46. Bulick AS, Munoz-Pinto DJ, Qu X, Mani M, Cristancho D, Urban M, et al. Impact of endothelial cells and mechanical conditioning on smooth muscle cell extracellular matrix production and differentiation. Tissue Eng Part A. 2009; 15(4):815–25. [PubMed: 19108675]
47. Fardin M, Rossier O, Rangamani P, Avigan P, Gauthier N, Vonnegut W, et al. Cell spreading as a hydrodynamic process. Soft Matter. 2010; 6(19):4788–99. [PubMed: 23908673]
48. Williams CG, Kim TK, Taboas A, Malik A, Manson P, Elisseeff J. In vitro chondrogenesis of bone marrow-derived mesenchymal stem cells in a photopolymerizing hydrogel. Tissue Eng. 2003; 9(4): 679–88. [PubMed: 13678446]
49. Browning MB, Dempsey D, Guiza V, Becerra S, Rivera J, Russell B, et al. Multilayer vascular grafts based on collagen-mimetic proteins. Acta Biomater. 2012; 8(3):1010–21. [PubMed: 22142564]
50. Yang T, Malkoch M, Hult A. The influence of diffusion time on the properties of sequential interpenetrating PEG hydrogels. J Polym Sci A1. 2013; 51(6):1378–86.
51. Nuttelman CR, Tripodi MC, Anseth KS. Synthetic hydrogel niches that promote hMSC viability. Matrix Biol. 2005; 24(3):208–18. [PubMed: 15896949]
52. Hassan W, Dong Y, Wang W. Encapsulation and 3D culture of human adipose-derived stem cells in an in-situ crosslinked hybrid hydrogel composed of PEG-based hyperbranched copolymer and hyaluronic acid. Stem Cell Res Ther. 2013; 4(2):32. [PubMed: 23517589]

53. Ingavle GC, Frei AW, Gehrke SH, Detamore MS. Incorporation of aggrecan in interpenetrating network hydrogels to improve cellular performance for cartilage tissue engineering. Tissue Eng Part A. 2013; 19(11–12):1349–59. [PubMed: 23379843]

54. Nguyen QT, Hwang Y, Chen AC, Varghese S, Sah RL. Cartilage-like mechanical properties of poly (ethylene glycol)-diacrylate hydrogels. Biomaterials. 2012; 33(28):6682–90. [PubMed: 22749448]

55. Cruise GM, Scharp DS, Hubbell JA. Characterization of permeability and network structure of interfacially photopolymerized poly(ethylene glycol) diacrylate hydrogels. Biomaterials. 1998; 19(14):1287–94. [PubMed: 9720892]

56. Helary C, Bataille I, Abed A, Illoul C, Anglo A, Louedec L, et al. Concentrated collagen hydrogels as dermal substitutes. Biomaterials. 2010; 31(3):481–90. [PubMed: 19811818]

57. Munoz-Pinto DJ, Jimenez-Vergara AC, Gelves LM, McMahon RE, Guiza-Arguello V, Hahn MS. Probing vocal fold fibroblast response to hyaluronan in 3D contexts. Biotechnol Bioeng. 2009; 104(4):821–31. [PubMed: 19718686]

58. Gao L, McBeath R, Chen CS. Stem cell shape regulates a chondrogenic versus myogenic fate through Rac1 and N-cadherin. Stem Cells. 2010; 28(3):564–72. [PubMed: 20082286]

59. Abbasi F, Mirzadeh H, Katbab AA. Sequential interpenetrating polymer networks of poly(2-hydroxyethyl methacrylate) and polydimethylsiloxane. J Appl Polym Sci. 2002; 85(9):1825–31.

60. Munoz-Pinto DJ, Bulick AS, Hahn MS. Uncoupled investigation of scaffold modulus and mesh size on smooth muscle cell behavior. J Biomed Mater Res A. 2009; 90A(1):303–16.

61. Nguyen QT, Hwang Y, Chen AC, Varghese S, Sah RL. Cartilage-like mechanical properties of poly (ethylene glycol)-diacrylate hydrogels. Biomaterials. 2012; 33(28):6682–90. [PubMed: 22749448]

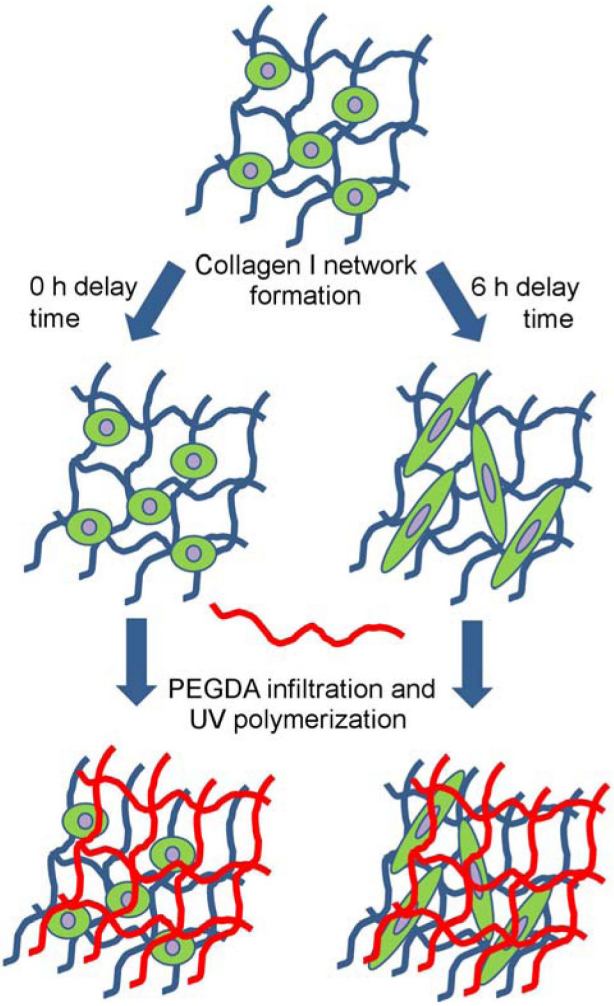

Figure 1.
Schematic representation of the sequential collagen-PEGDA IPN fabrication process.

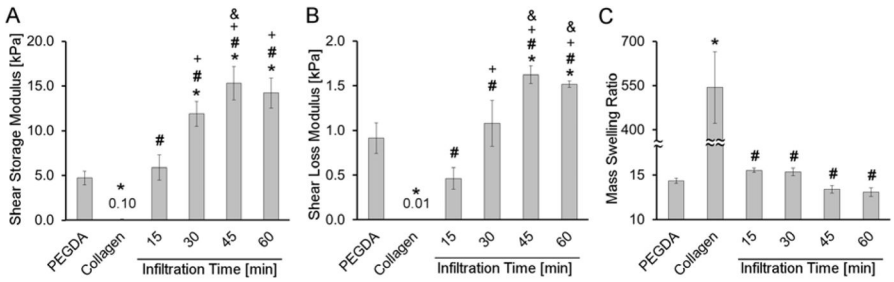

Figure 2.

Change in IPN rheological properties and swelling as a function of PEGDA infiltration time. (A) Shear storage modulus, (B) Shear loss modulus, (C) Mass swelling ratio. For each formulation, n = 3–6 independent samples were measured. * significantly different from the pure nominal 10 % w/v PEGDA hydrogel, $p < 0.05$; $^{\#}$ significantly different from the pure 3 mg/mL collagen hydrogel, $p < 0.05$; $^{+}$ significantly different from the 15 min infiltration time, $p < 0.05$; $^{\&}$ significantly different from the 30 min infiltration time, $p < 0.05$.

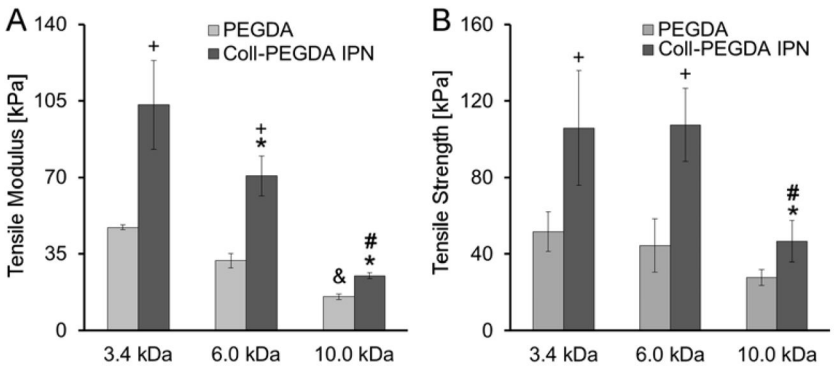

Figure 3.

Influence of PEGDA molecular weight on IPN tensile properties. (A) Tensile modulus, (B) Tensile strength. For each formulation, n = 3–5 independent samples were measured. * significantly different from the 3.4 kDa PEGDA IPN, $p < 0.05$; $^{\#}$ significantly different from 6.0 kDa PEGDA IPN, $p < 0.05$; $^{+}$ significantly different from the corresponding pure PEGDA control, $p < 0.05$; $^{\&}$ significantly different from the pure 3.4 kDa PEGDA hydrogel, $p < 0.05$.

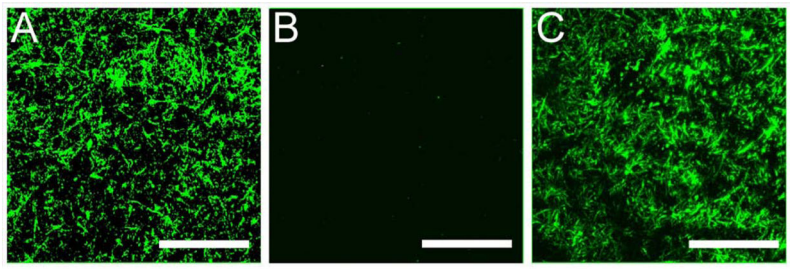

Figure 4.

Representative confocal images of a transverse section through hydrogels immunostained for collagen I: (A) a 3 mg/mL collagen hydrogel; (B) a nominal 10% w/v 6.0 kDa PEGDA hydrogel; (C) a 6.0 kDa PEGDA IPN hydrogel at 60 min infiltration time. Scale bar = 50 μm.

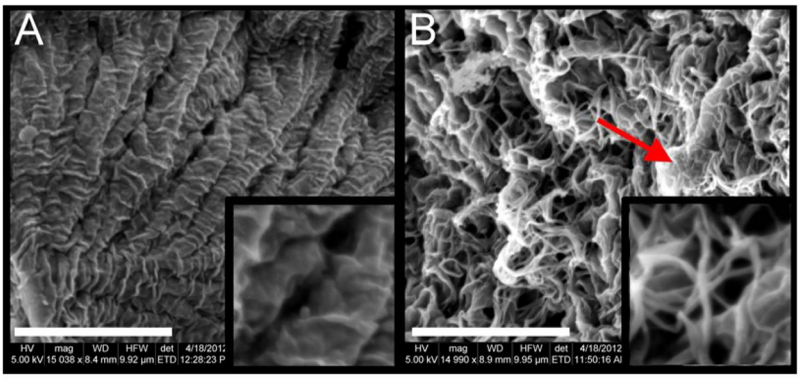

Figure 5.

Microscopy-based assessment of IPN microstructure. (A) A representative SEM image of a nominal 10% w/v 6.0 kDa PEGDA hydrogel control at 15,000X magnification, scale bar = 4 μm. The image inset shows the gel structure at 40,000X magnification; (B) A representative SEM image of a 6.0 kDa PEGDA IPN, 60 min infiltration time at 15,000X magnification, scale bar = 4 μm, arrow indicating a flat PEGDA structure surrounded by collagen fibrils. The image inset shows the gel structure at 40,000X magnification.

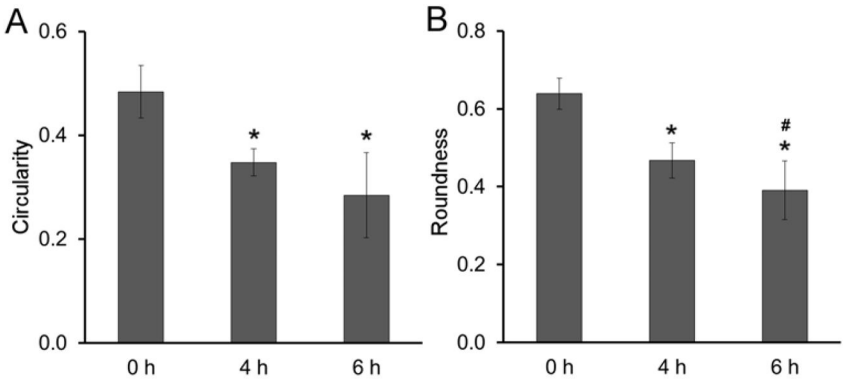

Figure 6.

Cell shape descriptors (A) Circularity, (B) Roundness in 6.0 kDa PEGDA IPN. Approximately 100 cells were evaluated for each time delay. * significantly different from the 0 h time delay samples, $p < 0.05$.

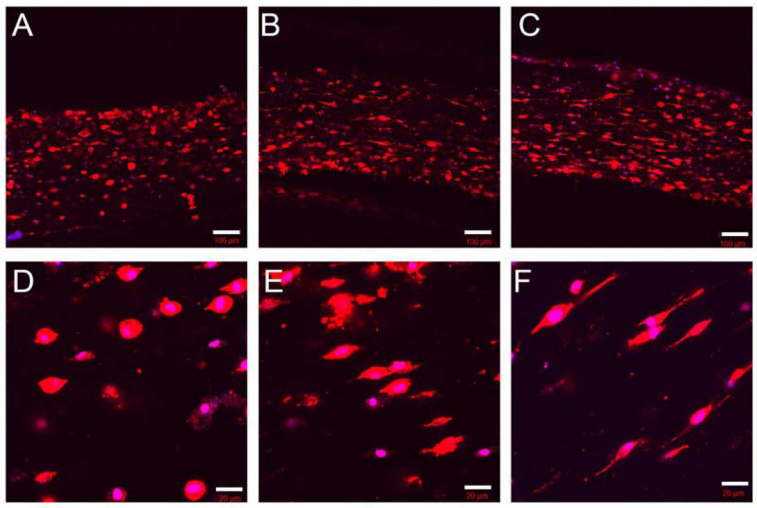

Figure 7.

Representative images of phalloidin-stained cells in collagen-PEGDA IPNs (3 mg/mL collagen, 6.0 kDa PEGDA) as a function of the delay time between collagen network formation and PEGDA infiltration. (A, D) 0 h delay time, (B, E) 4 h delay time, (C, F) 6 h delay time. The cell cytoskeleton is stained with rhodamine phalloidin, and the cell nuclei are stained with DAPI. The scale bars in (A, B, C) equal 20 μm and the scale bars in (D, E, F) equal 100 μm.

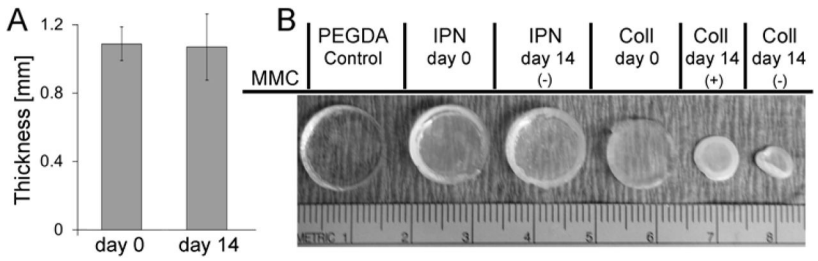

Figure 8.

Volume assessment of collagen-PEGDA IPNs (3 mg/mL collagen, 6.0 kDa PEGDA, 60 min infusion time) containing elongated MSCs over 14 days of culture. (A) Average IPN thickness at day 14 relative to day 0; (B) Representative images of day 0 and day 14 IPNs relative to pure PEGDA and pure collagen control gels.

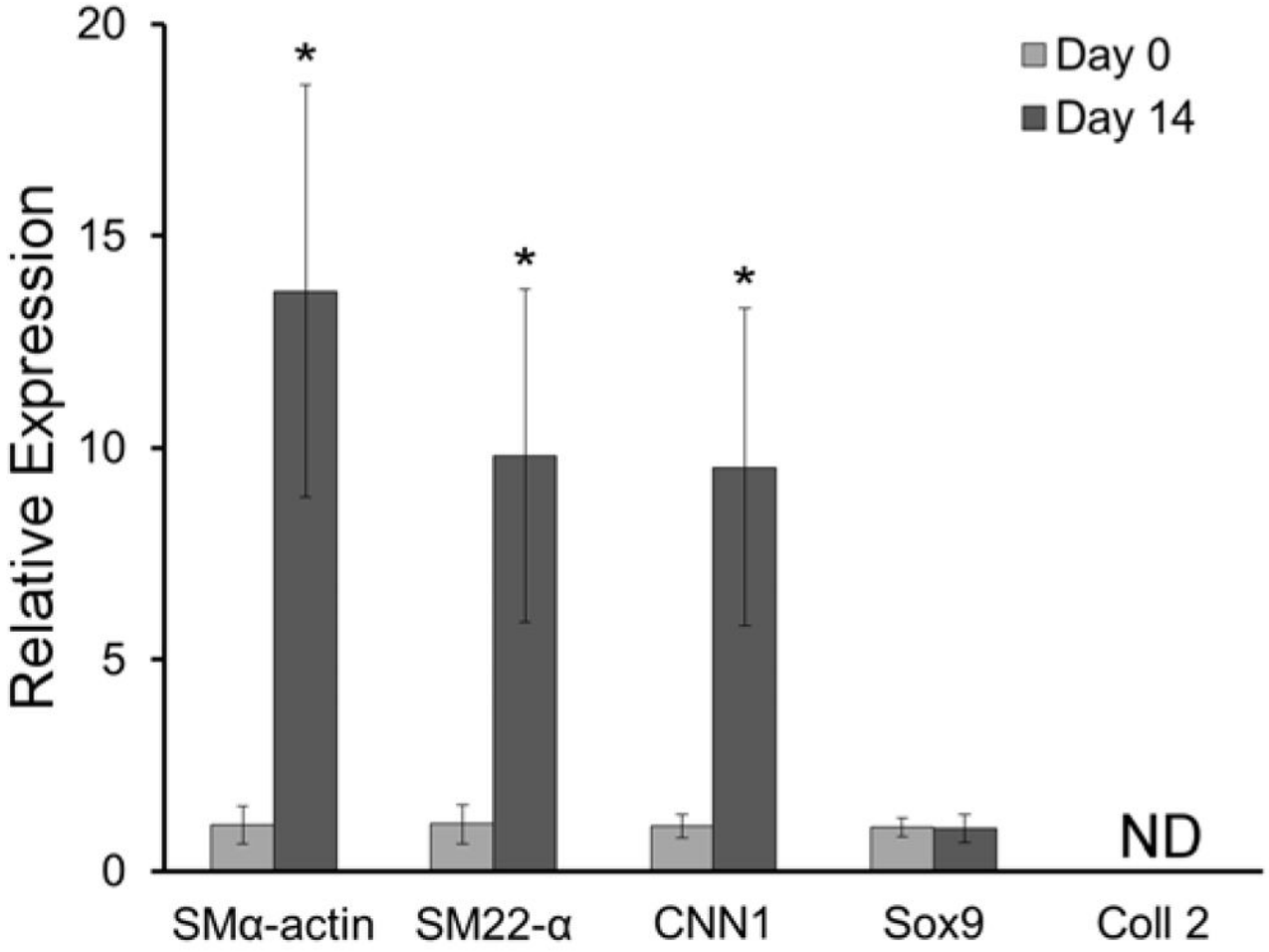

Figure 9.

Gene expression of SMα-actin, SM22-α, CNN1, sox9 and collagen II by elongated MSCs in a 6.0 kDa PEGDA IPN (60 min infusion time) following 14 days of culture relative to day 0. Gene expression was assessed relative to the housekeeping gene GAPDH and fold differences were calculated using the $\Delta\Delta C_t$ method. Four IPN discs were evaluated for each time point. * significantly different from day zero, $p < 0.05$.

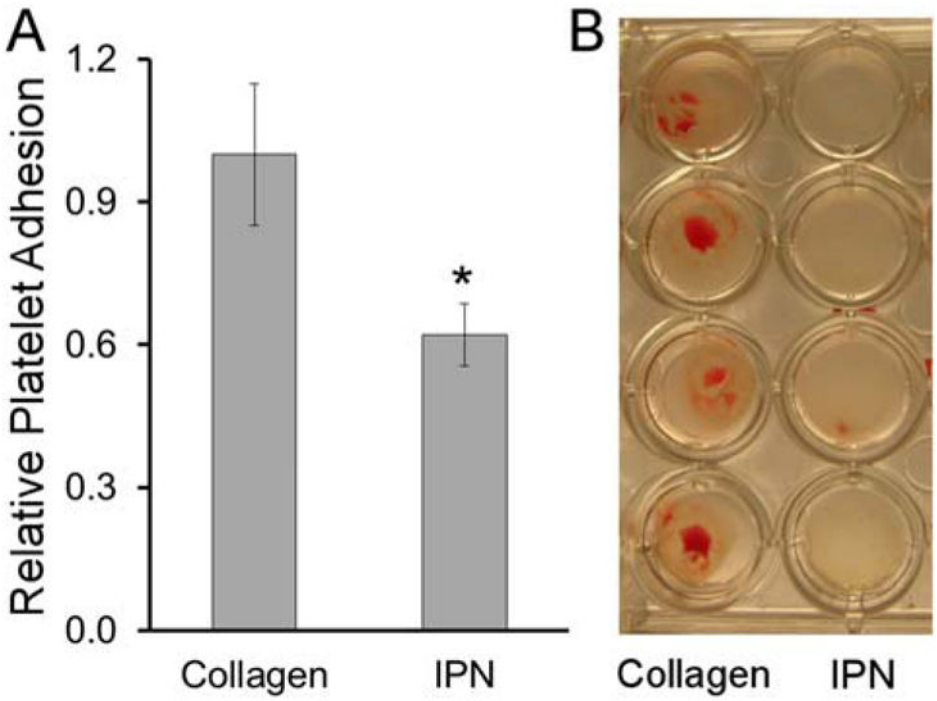

Figure 10.

Initial thrombogenicity assessment. (A) 6.0 kDa PEGDA IPN (60 min infusion time) platelet adhesion relative to collagen hydrogel positive controls, n = 4 samples per formulation. (B) Representative images of clot formation on various hydrogel surfaces.

Table 1

6 kDa PEGDA IPN tensile modulus and tensile strength as a function of infiltration time.

	Formulation	Tensile Modulus, E [kPa]	Tensile Strength, TS [kPa]
Controls	PEGDA 10 w/v% (nominal)	31.0 ± 4.2	46.1 ± 15.0
	Collagen 3 mg/ml	ND	ND
Infiltration Time [min]	15	37.2 ± 9.5	32.4 ± 15.3
	30	62.8 ± 4.3[a]	77.4 ± 14.6[b]
	45	78.6 ± 12.4[a,b]	120.7 ± 12.8[a,b,c]
	60	70.8 ± 9.0[a,b]	107.8 ± 19.1[a,b]

(ND) Not able to be determined with ring tension test;

[a] significantly different from nominal 10% w/v 6 kDa PEGDA, $p < 0.05$;

[b] significantly different from 15 min infiltration time, $p < 0.05$;

[c] significantly different from 30 min infiltration time, $p < 0.05$.

Table 2

Influence of PEGDA molecular weight on IPN shear storage, loss modulus and loss tangent.

Hydrogel	Shear Storage Modulus G′[kPa]	Shear Loss Modulus G″[kPa]	Loss tangent
3.4 kDa PEGDA	9.9 ± 1.9	2.0 ± 0.5	0.22 ± 0.06
3.4 kDa PEGDA IPN	16.9 ± 3.5[c]	2.0 ± 0.4[c]	0.12 ± 0.02[c]
6.0 kDa PEGDA	4.9 ± 0.8	0.9 ± 0.2	0.19 ± 0.06
6.0 kDa PEGDA IPN	14.2 ± 3.7[c]	1.6 ± 0.4[c]	0.11 ± 0.01[c]
10.0 kDa PEGDA	3.5 ± 0.6[d]	0.6 ± 0.2[d]	0.19 ± 0.06
10.0 kDa PEGDA IPN	7.8 ± 0.3[a,b,c]	0.7 ± 0.3[a,b]	0.09 ± 0.04[c]

[a] significantly different from 3.4 kDa PEGDA IPN, $p < 0.05$;

[b] significantly different from 6.0 kDa PEGDA IPN, $p < 0.05$;

[c] significantly different from corresponding PEGDA control, $p < 0.05$.

Table 3

Influence of collagen concentration on 6.0 kDa PEGDA IPN shear storage, loss modulus and loss tangent.

Collagen concentration [mg/mL]	Shear Storage Modulus G′ [kPa]	Shear Loss Modulus G″ [kPa]	Loss tangent
1.5	11.0 ± 4.6	1.2 ± 0.4	0.14 ± 0.02
3.0	14.2 ± 3.7	1.6 ± 0.4	0.12 ± 0.01
5.0	21.7 ± 4.1[a,b]	1.5 ± 0.3	0.07 ± 0.01[a,b]

[a] significantly different from 1.5 mg/mL IPN, $p < 0.05$;

[b] significantly different from 3.0 mg/mL IPN, $p < 0.05$.